J. Biochem. 2012;151(3):335–342 doi:10.1093/jb/mvr140

JB THE JOURNAL OF BIOCHEMISTRY

NMR and CD analysis of an intermediate state in the thermal unfolding process of mouse lipocalin-type prostaglandin D synthase

Received November 2, 2011; accepted December 12, 2011; published online December 30, 2011

Yuya Miyamoto[1,2], Yasuo Noda[3], Tsukimi Iida[4], Keisuke Yamaguchi[1], Shigenori Nishimura[1], Akiyoshi Tanaka[5], Shin-ichi Segawa[3] and Takashi Inui[1,*]

[1]Graduate School of Life and Environmental Sciences, Osaka Prefecture University, 1-1 Gakuen-cho, Naka-ku, Sakai, Osaka 599-8531; [2]Research Fellow of the Japan Society for the Promotion of Science, 8 Ichiban-cho, Chiyoda-ku, Tokyo 102-8472, [3]School of Science and Technology, Kwansei Gakuin University, 2-1 Gakuen, Sanda, Hyogo 669-1337; [4]Department of Food and Nutrition, Tsu City College, 157 Ishinden-Nakano, Tsu, Mie 514-0112; and [5]Graduate School of Bioresources, Mie University, 1577 Kurimamachiya-cho, Tsu, Mie 514-8507, Japan

*Takashi Inui, Graduate School of Life and Environmental Sciences, Osaka Prefecture University, 1-1 Gakuen-cho, Naka-ku, Sakai, Osaka 599-8531, Japan. Tel: +81-72-254-9473, Fax: +81-72-254-9921, email: inuit@bioinfo.osakafu-u.ac.jp

We previously reported that the thermal unfolding of mouse lipocalin-type prostaglandin D synthase (L-PGDS) is a completely reversible process under acidic conditions and follows a three-state pathway, including an intermediate state (I) between native state (N) and unfolded state. In the present study, we investigated the intermediate state of mouse C65A L-PGDS and clarified the local conformational changes in the upper and bottom regions by using NMR and CD spectroscopy. The ^{1}H-^{15}N HSQC measurements revealed that the backbone conformation was disrupted in the upper region of the β-barrel at 45°C, which is around the T_m value for the N ↔ I transition, but that the signals of the residues located at the bottom region of L-PGDS remained at 54°C, where the maximum accumulation of the intermediate state was found. ^{1}H-NMR and CD measurements showed that the T_m values obtained by monitoring Trp54 at the upper region and Trp43 at the bottom region of the β-barrel were 41.4 and 47.5°C, respectively, suggesting that the conformational change in the upper region occurred at a lower temperature than that in the bottom region. These findings demonstrate that the backbone conformation of the bottom region is still maintained in the intermediate state.

Keywords: conformational change/intermediate state/lipocalin-type prostaglandin D synthase/NMR spectroscopy/thermal unfolding.

Abbreviations: DSC, differential scanning calorimetry; HSQC, heteronuclear single quantum correlation; I, intermediate state; L-PGDS, lipocalin-type prostaglandin D synthase; N, native state; SAXS, small-angle X-ray scattering; U, unfolded state.

Lipocalin-type prostaglandin (PG) D synthase (L-PGDS, prostaglandin-H_2 D-isomerase; EC 5.3.99.2) is the key enzyme responsible for the formation of PGD_2, a potent endogenous somnogen and a nociceptive modulator as well as an allergic mediator, from PGH_2 (*1*). L-PGDS is abundantly expressed mainly in the central nervous system and male genital organs of various mammals (*1*). It is a member of the lipocalin superfamily (*2*). Lipocalins are small globular proteins that are found in bacteria, plants, invertebrates and vertebrates (*3*). Despite amino acid sequence identities that are often <20%, members of this family share a common fold comprising an eight-stranded anti-parallel β-barrel forming a hydrophobic cavity and an attached α-helix (*4*). The lipocalins play a role in the storage and transport of small lipophilic compounds such as vitamins, steroids and secondary metabolites (*5*). Some members of this family also have more specialized functions, for example in olfaction (*6*), invertebrate colouration (*7*), mediation of cell homoeostasis (*8*) and immune regulation (*9*). L-PGDS has also been shown to bind a large variety of lipophilic molecules such as retinoids, haem metabolites, thyroid hormones and amyloid-β peptides *in vitro* (*10–13*). Thus, L-PGDS is a multi-functional protein, acting as both a PGD_2 synthase and an extracellular transporter for small lipophilic molecules.

So far, a series of studies have been carried out in our group to investigate the structure–function relationship of L-PGDS. In terms of enzyme function, we showed that denaturant-induced unfolding of mouse L-PGDS is a reversible process and follows a four-state pathway including an activity-enhanced state at a low concentration of denaturants and an inactive intermediate state at a higher concentration of denaturants (*14*). The former state possesses a native-like tertiary structure, and the latter has the core secondary structure (*14*). In terms of transporter function, using NMR spectroscopy we observed that mouse C65A L-PGDS, which has alanine in place of a catalytic residue of cysteine, has a typical lipocalin fold with an eight-stranded anti-parallel β-barrel (*15*). The combination of small-angle X-ray scattering (SAXS) and NMR spectroscopy revealed that the conformation of the upper region of the β-barrel changes upon binding a lipophilic molecule and then L-PGDS becomes compact (*15*, *16*). This directly demonstrates the structural flexibility of mouse L-PGDS.

We have also investigated the folding and unfolding mechanism of mouse L-PGDS to understand the relationship between structure and stability. Differential

scanning calorimetry (DSC) and CD measurements revealed that under acidic conditions (pH 4.0), the thermal unfolding of mouse C65A L-PGDS without PGDS activity is also a completely reversible process, and we proposed a three-state unfolding between the native state (N) and the unfolded state (U) through an intermediate state (I) in which L-PGDS still maintained a significant amount of the secondary structure (*17*). The transition temperatures (T_m) for the N ↔ I and I ↔ U transitions were far apart, 48.0 and 60.8°C, respectively (*17*). Thus, L-PGDS is particularly interesting because it has multiple functions and a multi-state equilibrium unfolding.

It often happens that proteins fold and unfold with a complicated equilibrium where intermediates accumulate (*18–21*). It is essential for the understanding of the protein unfolding mechanism to investigate the conformational changes and intermediate structure during protein unfolding. Although the detailed structures and energetic properties of intermediates are difficult to probe due to their instability and low population, the intermediate state in the protein unfolding has been characterized in recent years using NMR spectroscopy (*22*, *23*).

In this study, we investigated the intermediate state of mouse C65A L-PGDS on its structural basis by using NMR and CD spectroscopy to characterize the thermal unfolding process of this protein in detail. The combination of NMR and CD spectroscopy is a powerful tool for detailed characterization of local and global conformational changes and protein structure associated with protein unfolding. To investigate the local conformational change in the bottom region of the β-barrel of L-PGDS in the thermal unfolding process, we measured the CD spectra of the W54F/C65A mutant.

Materials and Methods

Protein preparations

We used mouse recombinant C65A L-PGDS, in which a catalytic residue of cysteine has been replaced with alanine, to prevent formation of incorrect disulphide bonds. We also used the W54F/C65A mutant which has the Trp43 residue located at the bottom region of the β-barrel and has the Phe54 residue instead of the Trp54 residue at the upper region of the β-barrel (*14*). These proteins were expressed as a glutathione *S*-transferase fusion protein in *Escherichia coli* BL21(DE3) (TOYOBO, Tokyo, Japan) as described previously (*12*). The fusion protein was bound to glutathione-Sepharose 4B (GE Healthcare Bio-Sciences, Little Chalfont, UK) and incubated with thrombin (Sigma Chemical Co., St Louis, MO, USA, 100 U/100 μl) to release the L-PGDS. The recombinant protein was further purified by size-exclusion chromatography as described previously (*14*). Then, the purified proteins were dialysed against 20 mM sodium acetate at pH 4.0. The protein concentration was determined spectroscopically using the molar extinction coefficient at 280 nm, $\varepsilon_{280} = 23{,}000\ M^{-1}cm^{-1}$ for C65A L-PGDS and $\varepsilon_{280} = 17{,}600\ M^{-1}cm^{-1}$ for the W54F/C65A mutant.

NMR analysis

Uniformly ^{15}N-labelled protein was prepared by growing *E. coli* in M9 minimal medium containing $^{15}NH_4Cl$ (1 g/l) as sole nitrogen source (*14*, *15*). Non-labelled and ^{15}N-labelled proteins were used for the 1D ^1H-NMR and the 2D ^1H-^{15}N heteronuclear single quantum correlation (HSQC) measurements, respectively. All NMR samples were prepared at 0.3 mM in 20 mM sodium acetate-*d4* of 90% H_2O/10% D_2O mixture at pH 4.0. The NMR experiments were performed on a Bruker Avance 600 DRX spectrometer (Bruker BioSpin, Rheinstetten, Germany) over a temperature range from 25 to 82°C. Sodium 2,2-dimethyl-2-silapentane-5-sulphonate was used as an external reference of ^1H chemical shifts. ^{15}N chemical shifts were indirectly calibrated from the gyromagnetic ratio (*24*). All the NMR spectra were processed and analysed using the NMRPipe (*25*) and Sparky (Goddard, T.D. and Kneller, D.G., SPARKY 3, University of California, San Francisco, USA).

The ratio of NMR peak intensities at different temperatures was analysed on the two-component theory (state i ↔ state j). Thermodynamic parameters such as van't Hoff enthalpy change $\Delta H(T_m)$ and transition temperature T_m were determined by fitting to the van't Hoff equation:

$$K = \frac{I_j}{I_i} \tag{1}$$

$$\left(\frac{\partial \ln K}{\partial (1/T)}\right)_P = -\frac{\Delta H(T_m)}{R} \tag{2}$$

where K denotes the equilibrium constant, I represents the observed intensity of the peak at varied temperatures, and I_i and I_j are the intensities of state i and state j, respectively.

CD analysis

The near-UV and far-UV CD spectra were measured with a spectropolarimeter, model J-820 (Jasco, Tokyo, Japan), equipped with a Peltier PTC-423 L thermo-unit (Jasco), using optical quartz cuvettes with 10 and 1.0 mm path lengths, respectively. The final protein concentrations were 50 and 5 μM for near-UV and far-UV CD measurements, respectively. As for thermal unfolding experiments, changes in the CD intensities were measured at 290 and 200 nm over a temperature range from 20 to 90°C at a scan rate of 1°C/min. The path length of the optical cuvette was 10 mm. The final protein concentrations were 50 and 0.5 μM for the measurements at 290 and 200 nm, respectively. The thermal unfolding curves were analysed using the two-state model (state i ↔ state j) as described earlier (*17*). Molar ellipticity at each temperature was represented by the following equation:

$$\theta_{obs} = \frac{\theta_i + \theta_j exp(-\Delta G(T)/RT)}{1 + exp(-\Delta G(T)/RT)} \tag{3}$$

where $\Delta G(T)$ is the difference in free energy between the states i and j. The ellipticities characteristic for each state were assumed to be a linear function of temperature:

$$\theta(T) = \theta_0 + kT \tag{4}$$

The Gibbs free energy $\Delta G(T)$ was represented as a function of temperature:

$$\Delta G(T) = \Delta H(T_m)\left(1 - \frac{T}{T_m}\right) - \Delta C_p\left((T_m - T) + T\ln\frac{T}{T_m}\right) \tag{5}$$

where $\Delta H(T_m)$ and ΔC_p are the van't Hoff enthalpy change at the transition temperature and the difference in heat capacity before and after the thermal unfolding, respectively. The thermodynamic parameters were estimated in global fits based on experimental points by nonlinear least-squares analysis using the Levenberg–Marquardt algorithm.

Results

Thermal unfolding process of C65A L-PGDS characterized by multi-dimensional NMR measurements

In a previous study, we proposed that the thermal unfolding of mouse C65A L-PGDS follows a three-state pathway, including an intermediate state (I) between native state (N) and unfolded state (U) (*17*). In this study, we investigated this intermediate state using NMR spectroscopy. Figure 1 shows the ^1H-^{15}N HSQC spectra of C65A L-PGDS at pH 4.0 and 25, 39, 45 and 54°C. The cross-peaks of C65A L-PGDS at 25°C were well dispersed, which is characteristic for a folded protein; the cross-peaks were previously assigned by means of multi-dimensional NMR

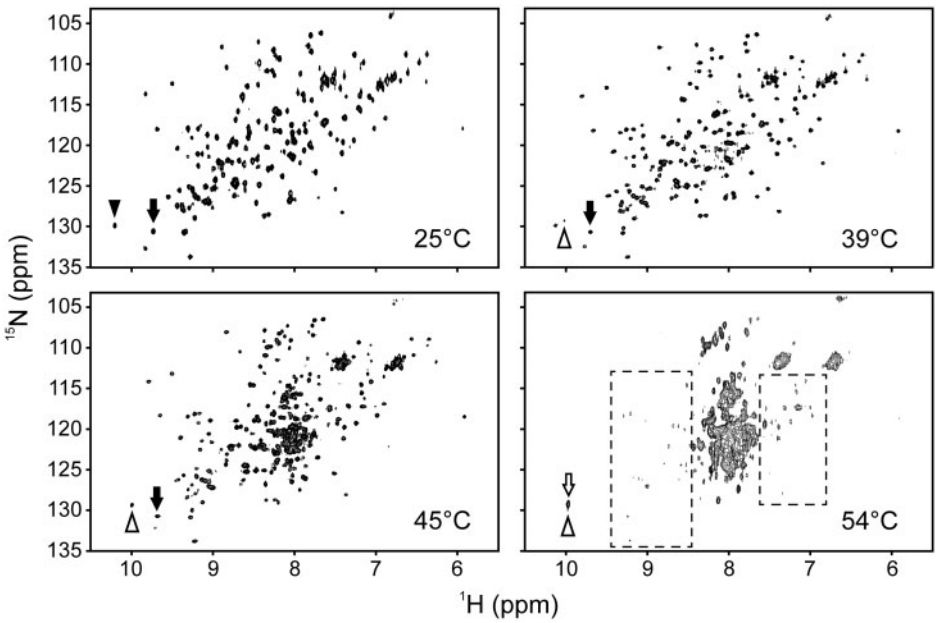

Fig. 1 Temperature dependence of ^{1}H-^{15}N HSQC spectra of C65A L-PGDS. All spectra were recorded at various temperatures between 25°C and 54°C as marked inside the individual panels. Dashed boxes indicate cross-peaks around 7 and 9 ppm that are observed at chemical shifts similar to those of the native state at 54°C. The εNH cross-peaks of Trp54 and Trp43 for the folded protein are indicated by a black arrowhead and a black arrow, respectively. The new cross-peaks of Trp54 and Trp43 for the second species are indicated by a white arrowhead and a white arrow, respectively.

spectroscopy (*15*). With increasing temperature, induced chemical shift changes and/or signal broadening were observed for some cross-peaks (Fig. 1). The observed signals at 45°C, which is around the T_m value for the N ↔ I transition obtained by DSC and CD measurements (*17*), could be assigned by careful comparison of the HSQC spectra obtained at 25, 35, 39, 43 and 45°C (Supplementary Table SI). Above 45°C, however, most of the cross-peaks could not be assigned due to overlap or signal broadening. In order to quantify the observed chemical shift changes during the N ↔ I transition, we calculated the magnitude of the composite ^{1}H and ^{15}N chemical shift changes caused by increasing temperature from 25 to 45°C (Fig. 2A). At 45°C, 10% of the signals (17 of 167 cross-peaks) showed chemical shift changes larger than 0.14 ppm (Fig. 2A, colored in blue). Mapping these residues onto the solution structure of C65A L-PGDS (PDB code: 2RQ0) (*15*) revealed that they were located near aromatic side-chains (Fig. 2B and C), suggesting changes in the aromatic side-chain interactions of L-PGDS. Furthermore, 10% of the signals (16 of 167) disappeared from the ^{1}H-^{15}N HSQC spectrum at 45°C, and these missing residues were located in the upper region of the β-barrel (Fig. 2B, colored in red), indicating the presence of exchanges between multiple conformations on the NMR time scale in the N ↔ I transition. We therefore concluded that the conformational changes occurred in the upper region of L-PGDS in the N ↔ I transition.

Although the ^{1}H-^{15}N HSQC spectrum of C65A L-PGDS showed limited chemical shift dispersion at 54°C, where the maximum accumulation of the intermediate was found by DSC measurements (*17*), 13% of the signals (22 of 167) around 7 and 9 ppm in the ^{1}H dimension were still observed at chemical shifts similar to those of the native state (Fig. 1, dashed boxes). These residues were located at the bottom region of the β-barrel (Fig. 2D), indicating that the backbone conformation of the bottom region was still maintained in the intermediate state.

Thermal transition of upper region of β-barrel characterized by 1D ^{1}H-NMR measurements

We measured 1D ^{1}H-NMR spectra of C65A L-PGDS over a wide temperature range. Figure 3 displays the amide and aromatic regions of 1D ^{1}H-NMR spectra of C65A L-PGDS at temperatures from 25°C to 82°C. As shown in Fig. 3, the ^{1}H-NMR spectra at temperatures higher than 60°C show a disruption of the tertiary structure of C65A L-PGDS. After heating to 82°C and cooling down to 35°C, the ^{1}H-NMR spectrum of C65A L-PGDS was completely identical to that prior to heating (Supplementary Fig. S1), indicating that the thermal unfolding of C65A L-PGDS is a completely reversible process at the atomic level. Thus, it is possible to apply equilibrium thermodynamic analysis to the thermal unfolding of C65A L-PGDS.

Mouse L-PGDS contains two tryptophan residues, Trp43 and Trp54, which are located at the bottom and upper region of the β-barrel, respectively (Fig. 2C). In the ^{1}H-NMR spectrum at 25°C, an indole side-chain εNH peak of Trp54 for the folded protein was observed at 10.22 ppm (Fig. 3, black arrowhead) and is well separated from the main spectral envelope. This aspect of the spectrum therefore enables us to investigate the thermal unfolding process in the upper region of the β-barrel in detail. The εNH peak intensity of Trp54 for the folded protein gradually decreased with increasing temperature, and was reduced to noise level

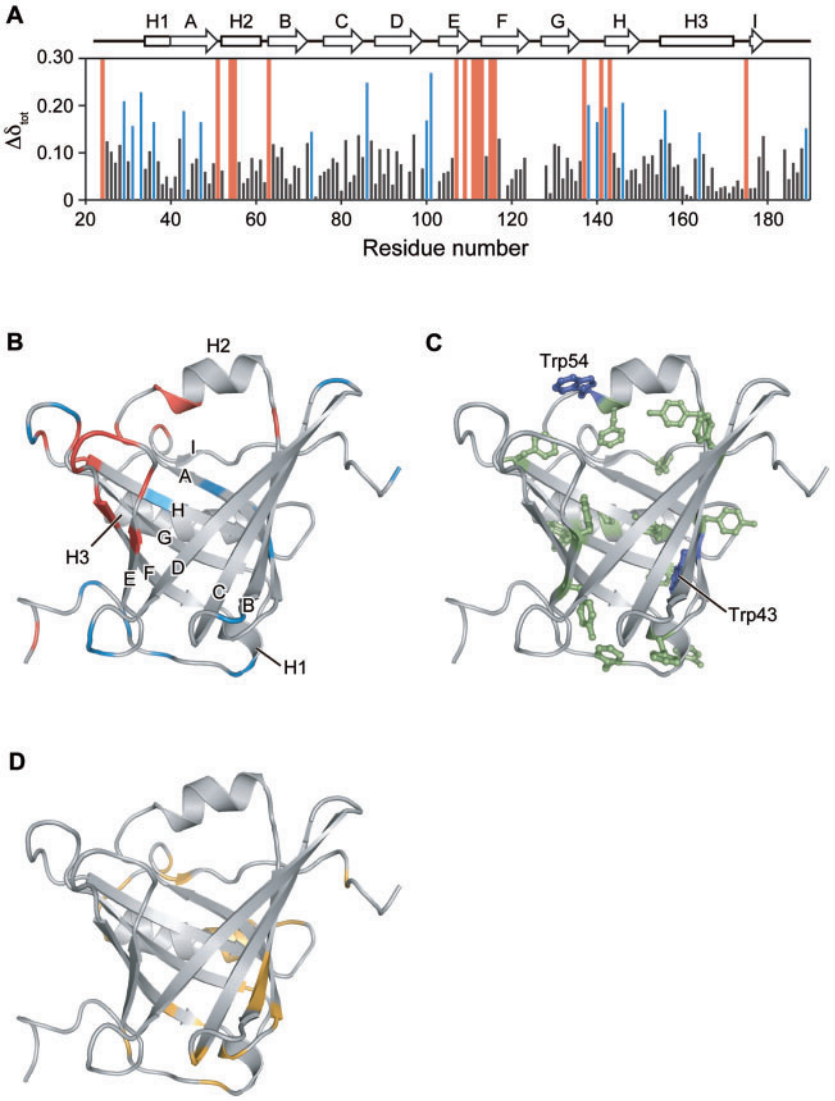

Fig. 2 Chemical shift changes during thermal unfolding of C65A L-PGDS. (A) The composite chemical shift changes ($\Delta\delta_{tot}$) between 25 and 45°C are plotted versus residue number. The $\Delta\delta_{tot}$ values were calculated using the equation, $\Delta\delta_{tot} = (\Delta\delta_{HN}^2 + \Delta\delta_N^2/25)^{1/2}$, where $\Delta\delta_{HN}$ and $\Delta\delta_N$ are the chemical shift changes of the amide proton and nitrogen, respectively. The residues with large chemical shift changes ($\Delta\delta_{tot} > 0{\cdot}14$ ppm) are shown as blue bars. The residues with cross-peaks disappearing at 45°C are indicated by red boxes. Secondary structure elements are indicated by arrows for β-strands and rectangles for helices. (B) Mapping of the residues indicated in (A) on C65A L-PGDS solution structure (PDB code: 2RQ0). The residues with large chemical shift changes ($\Delta\delta_{tot} > 0.14$ ppm) and with cross-peaks disappearing at 45°C are colored in blue and red, respectively. (C) Structural position of the aromatic residues in C65A L-PGDS. Two tryptophan residues are labelled and shown as dark blue sticks. All phenylalanine and tyrosine residues are shown as green sticks. (D) Mapping of the residues whose cross-peaks remained at 54°C on C65A L-PGDS solution structure. These residues are colored in orange. Graphical representations were prepared using PyMOL (*32*).

at temperatures higher than 50°C. On the other hand, above 35°C, a new broad εNH peak of Trp54 for the second species emerged at the high field side of that for folded C65A L-PGDS (Fig. 3, white arrowhead), and then sharpened and intensified with increasing temperature. Figure 4A shows the ratio of these Trp54 εNH peak intensities at different temperatures. Then we estimated the thermodynamic parameters for the transition by van't Hoff analysis [Equations (1 and 2) in 'Materials and Methods' section] (Fig. 4B). The T_m and van't Hoff enthalpy change [$\Delta H(T_m)$] for the thermal transition obtained by monitoring Trp54 εNH peaks were 41.4 ± 0.3°C and 273 ± 21 kJ/mol, respectively. We observed that the HSQC cross-peak of Trp43 for the folded protein (Fig. 1, black arrow) had a chemical shift different from that of the second species (Fig. 1, 54°C, white arrow), and that the Trp43 εNH cross-peak for the folded protein at 45°C was with intensity similar to that at 25°C. Forty-five degree is higher than the transition temperature obtained by monitoring the εNH peak of Trp54 (41.4°C). Therefore, we believe that there is no signal overlap effect in the transition region shown in Fig. 4B.

Thermal transition of bottom region of β-barrel in W54F/C65A mutant characterized by CD spectroscopy

In order to investigate the thermal unfolding process in the bottom region of the β-barrel, we measured the CD spectra of the W54F/C65A mutant, which contains a tryptophan residue of Trp43 located at the bottom region of the β-barrel.

The near-UV CD spectrum of the native state for the W54F/C65A mutant at 20°C exhibited a large negative Cotton effect at 290 nm, and was similar to that of C65A L-PGDS (Fig. 5A), suggesting that Trp54 does not contribute to negative ellipticity at 290 nm. We therefore could assign the large negative Cotton effect at 290 nm to Trp43. The far-UV spectrum of the native state for the W54F/C65A mutant at 20°C showed a spectrum with an abundance of β-sheet structure and was also similar to that for C65A L-PGDS (Fig. 5B), suggesting that the replacement of Trp54 with phenylalanine did not significantly affect the secondary structure of L-PGDS. Trp43 is therefore a probe for monitoring local conformational changes in the bottom region of this protein. Figures 5C and D show the equilibrium transition curve of the W54F/C65A mutant monitored at 290 and 200 nm, at which wavelength the change in ellipticity was larger (Supplementary Fig. S2). The values of T_m and $\Delta H(T_m)$ were obtained by fitting according to Equations (*3*–*5*) in 'Materials and Methods' section. Fitting the data to a model for two-state equilibrium unfolding provided a T_m of 47.5 ± 0.1°C and a $\Delta H(T_m)$ of 260 ± 16 kJ/mol for the transition at 290 nm, and a T_m of 53.3 ± 0.4°C and a $\Delta H(T_m)$ of 180 ± 11 kJ/mol at 200 nm, summarized in Table I. The fitting curves calculated with these parameters are shown as solid lines in Fig. 5. These results indicate that the changes in the side-chain conformation of Trp43 monitored at 290 nm occurred at a temperature lower than the transition temperature of those in the backbone conformation monitored at 200 nm. The thermodynamic parameters for the unfolding of the W54F/C65A mutant are comparable to those of C65A L-PGDS described previously (*17*).

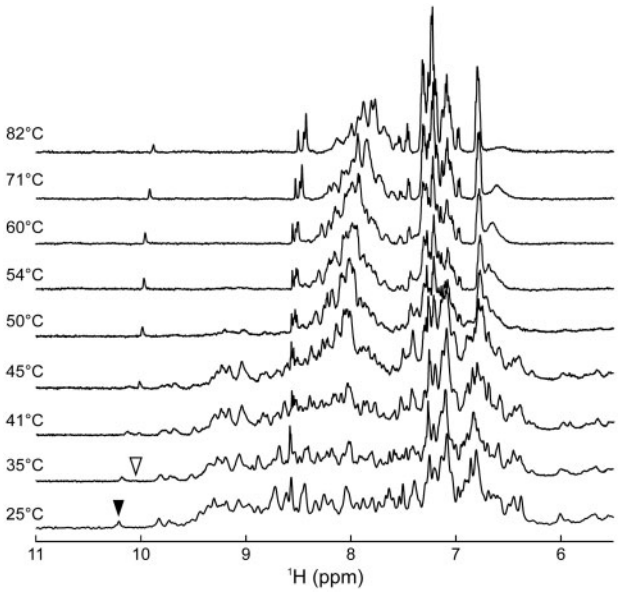

Fig. 3 Temperature dependence of 1D ^{1}H-NMR spectra of C65A L-PGDS. Temperatures are indicated adjacent to each spectrum. The εNH peak of Trp54 for the folded protein at 25°C is indicated by a black arrowhead. A new broad peak for the second species at 35°C is indicated by a white arrowhead.

Discussion

In the present study, we investigated local conformational change in the bottom region of the W54F/C65A mutant during the thermal unfolding process by using CD spectroscopy. CD measurements revealed that the replacing Trp54 with phenylalanine did not significantly affect the whole structure of L-PGDS in the native state (Fig. 5A and B). DSC measurements revealed that the thermal unfolding of the W54F/C65A mutant as well as C65A L-PGDS followed a three-state unfolding process involving an intermediate state, and that the thermodynamic parameters for unfolding of the W54F/C65A mutant were comparable with those of C65A L-PGDS described previously (*17*) (Table II and Supplementary Fig. S3). From these results, we expected that the W54F/C65A mutant could serve as a good model for studying the conformational changes in the bottom region of L-PGDS upon thermal unfolding by monitoring the anisotropic change of Trp43 in the CD measurements at 290 nm. Then, the CD data revealed that the T_m and $\Delta H(T_m)$ values were 47.5°C and 260 kJ/mol for the W54F/C65A mutant, showing good agreement with those for C65A

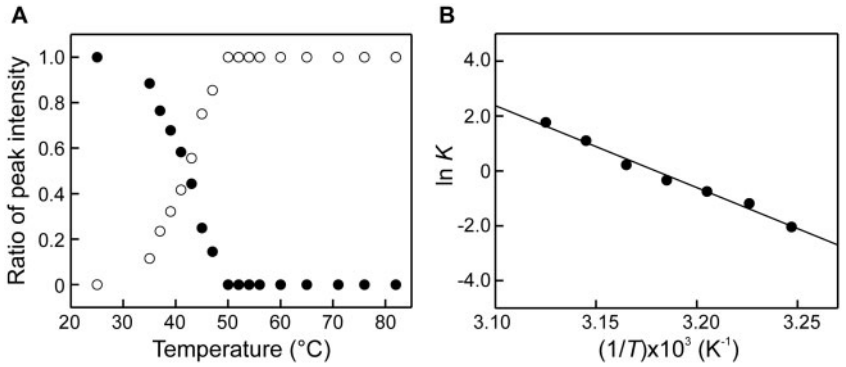

Fig. 4 Thermal transition monitored by Trp54 εNH peaks of C65A L-PGDS. (A) Ratio of the Trp54 peak intensities for the folded and second species noted in Fig. 3 are shown by black and white circles, respectively. (B) van't Hoff plot for the thermal unfolding curve of Trp54 εNH peaks in (A) during the transition region. The line represents the linear least-squares fit of the experimental data.

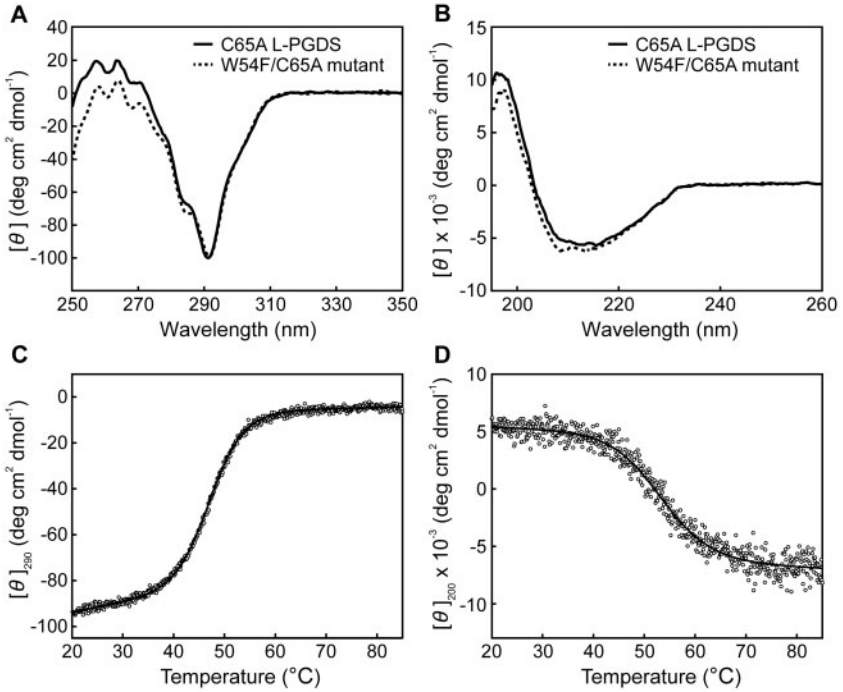

Fig. 5 Thermal unfolding of the W54F/C65A mutant monitored by near-UV and far-UV CD. (A) Near-UV (250–350 nm) and (B) far-UV (190–260 nm) CD spectra of C65A L-PGDS (solid line) and W54F/C65A (dashed line) at 20°C and pH 4.0. (C and D) Thermal unfolding curves of the W54F/C65A mutant. The unfolding transition was monitored by CD measurement at 290 (C) and 200 nm (D). The curves are the fitting curves based on experimental points by nonlinear least-squares analysis for the two-state transition.

Table I. Thermodynamic parameters obtained by CD measurements for unfolding of the W54F/C65A mutant and C65A L-PGDS.

	W54F/C65A mutant		C65A L-PGDS[a]	
Wavelength (nm)	T_m (°C)	$\Delta H(T_m)$ (kJ/mol)	T_m (°C)	$\Delta H(T_m)$ (kJ/mol)
290	47.5 ± 0.1	260 ± 16	46.9 ± 0.1	262 ± 6
200	53.3 ± 0.4	180 ± 11	54.6 ± 0.4	128 ± 6

T_m and ΔH denote transition temperature and enthalpy change, respectively.
[a]Iida *et al.*, 2008 (*17*).

Table II. Thermodynamic parameters obtained by DSC measurements for unfolding of the W54F/C65A mutant and C65A L-PGDS.

	W54F/C65A mutant		C65A L-PGDS[a]	
Step	T_m (°C)	$\Delta H(T_m)$ (kJ/mol)	T_m (°C)	$\Delta H(T_m)$ (kJ/mol)
N ↔ I	50.5 ± 0.1	257 ± 1	48.0 ± 0.1	206 ± 2
I ↔ U	62.4 ± 0.1	186 ± 1	60.8 ± 0.1	163 ± 2

T_m and ΔH denote transition temperature and enthalpy change, respectively, from native to intermediate state and from intermediate to unfolded state.
[a]Iida *et al.*, 2008 (*17*).

L-PGDS [$T_m = 46.9$°C and $\Delta H(T_m) = 262$ kJ/mol] (*17*). This result indicates that the thermal transition in the side-chain conformation of Trp43 at the bottom region of L-PGDS corresponds to the N ↔ I transition of the whole protein.

We used 1D ^{1}H-NMR to monitor the thermal unfolding transition of L-PGDS at the upper region of the β-barrel. The T_m and $\Delta H(T_m)$ values obtained by monitoring the Trp54 εNH peak were 41.4°C and 273 kJ/mol. This $\Delta H(T_m)$ value was in good agreement with the one obtained in the N ↔ I transition process by DSC and CD measurements (*17*), but the T_m value was lower. Local variations in thermal unfolding are part of the N ↔ I transition, and consequently the

conformational change in the upper region of the β-barrel occurs at a lower temperature than that in the bottom region. This idea is supported by a thermal unfolding study of ribonuclease (RNase) T1 elucidated using NMR spectroscopy (*26*). Singular value decomposition analysis based on ^{1}H-^{15}N HSQC spectra revealed that the thermal unfolding of RNase T1 could be described by a two-state transition model, and ^{1}H-^{1}H NOE analysis showed that the helical region starts to unfold at a lower temperature than some β-strands. This report indicates that the two state transition of RNase T1 appears to involve locally different conformational changes. In our case, ^{1}H-^{15}N HSQC measurements revealed that the backbone conformation was disrupted in the upper region of the β-barrel at 45°C, which is around the T_m value for the N ↔ I transition (Fig. 2B). This result suggests that a locally different conformational change such as the conformational change in the upper region of the β-barrel is also involved in the N ↔ I transition of L-PGDS.

In this study, we also characterized the backbone intermediate structure of C65A L-PGDS using NMR spectroscopy. The ^{1}H-^{15}N HSQC measurements revealed that the backbone cross-peaks of the residues located at the bottom region of the β-barrel in the intermediate state were still observed at chemical shifts similar to those of the native state (Figs 1 and 2D). Our previous experiments based on CD measurements revealed that the aromatic side-chain conformation in the intermediate state was different from that in the native state, while a significant amount of secondary structure remained (*17*). Considering all these lines of evidence, we conclude that although the aromatic side-chain interactions and the conformation in the upper region are disrupted in the intermediate state, L-PGDS possesses a well-organized backbone structure in the bottom region.

β-Lactoglobulin, another member of the lipocalin superfamily, folds through a unique pathway with non-native intermediates (*27*–*30*). In the case of bovine β-lactoglobulin, hydrogen exchange experiments revealed that an early folding intermediate had the native-like structure at F–H strands and the C-terminal helix and that the non-native helices were formed in A–D strands (*27*, *28*). In the case of equine β-lactoglobulin, proline scanning mutagenesis revealed that, in the acid-denatured state which is an equilibrium analogue of an early folding intermediate of this protein, the H-strand region assumed a non-native helix in addition to the native-like C-terminal helix, whereas the F and G strands assumed a native-like β-hairpin (*30*). Equine β-lactoglobulin also has a partially folded state that manifests below 0°C in 2 M urea, with non-native helices at F, G and H strands in addition to the native-like C-terminal helix (*30*, *31*). These intermediate states and the partially folded state of β-lactoglobulin differ from the thermal unfolding intermediate state of L-PGDS in that these states of β-lactoglobulin possess not only partially native structures but also non-native helices, despite belonging to the same protein family. Thus, it is fundamentally important for both theoretical and applied aspects to investigate the structure–function relationships of each individual lipocalin protein under different conditions.

We have already reported that the upper region of C65A L-PGDS plays an important role in ligand binding (*15*). The NMR and SAXS studies revealed that after binding biliverdin, a lipophilic small molecule, conformational changes occurred in the upper region of C65A L-PGDS in EF-loop and H2-helix, indicating that such structural flexibility is related not only to a proper interaction between L-PGDS and the lipophilic molecule, but also to an ability to bind a variety of ligands (*15*). In addition, our fluorescence quenching assay showed that the intermediate state of C65A L-PGDS retained binding ability for biliverdin during the thermal unfolding process (T. Iida and T. Inui, unpublished results). Thus, the bottom structure of the β-barrel in L-PGDS is considered to be a minimal architecture for ligand binding as a transporter protein.

Supplementary Data

Supplementary Data are available at *JB* Online.

Acknowledgements

We thank Dr Joseph Rodrigue for critical reading of the article. We also thank Mrs Kaoru Saruwatari and Mizuki Tabata for their technical assistance. We also thank the Satellite Venture Business Laboratory of Mie University for use of a VP-DSC instrument.

Funding

Grants-in-Aid for Scientific Researches (B) and (C) (Grants 17300165 and 21500428 to T.I.), respectively; Grant-in-Aid for Scientific Research on Innovative Areas (Grant 21200076 to T.I.); Grant-in-Aid for JSPS Fellows (Grant 09J10176 to Y.M.); Osaka Prefecture University Special Research Grant (to T.I.).

Conflict of interest

None declared.

References

1. Urade, Y., and Hayaishi, O. (2000) Biochemical, structural, genetic, physiological, and pathophysiological features of lipocalin-type prostaglandin D synthase. *Biochim. Biophys. Acta.* **1482**, 259–271
2. Toh, H., Kubodera, H., Nakajima, N., Sekiya, T., Eguchi, N., Tanaka, T., Urade, Y., and Hayaishi, O. (1996) Glutathione-independent prostaglandin D synthase as a lead molecule for designing new functional proteins. *Protein Eng.* **9**, 1067–1082
3. Akerstrom, B., Flower, D.R., and Salier, J.P. (2000) Lipocalins: unity in diversity. *Biochim. Biophys. Acta.* **1482**, 1–8
4. Flower, D.R., North, A.C., and Sansom, C.E. (2000) The lipocalin protein family: structural and sequence overview. *Biochim. Biophys. Acta.* **1482**, 9–24
5. Flower, D.R. (1996) The lipocalin protein family: structure and function. *Biochem. J.* **318**, 1–14
6. Barbour, J., Neuhaus, E.M., Piechura, H., Stoepel, N., Mashukova, A., Brunert, D., Sitek, B., Stuhler, K., Meyer, H.E., Hatt, H., and Warscheid, B. (2008) New insight into stimulus-induced plasticity of the

olfactory epithelium in Mus musculus by quantitative proteomics. *J. Proteome Res.* **7**, 1594–1605
7. Chayen, N.E., Cianci, M., Grossmann, J.G., Habash, J., Helliwell, J.R., Nneji, G.A., Raftery, J., Rizkallah, P.J., and Zagalsky, P.F. (2003) Unravelling the structural chemistry of the colouration mechanism in lobster shell. *Acta Crystallogr. D Biol. Crystallogr.* **59**, 2072–2082
8. Mucha, M., Skrzypiec, A.E., Schiavon, E., Attwood, B.K., Kucerova, E., and Pawlak, R. (2011) Lipocalin-2 controls neuronal excitability and anxiety by regulating dendritic spine formation and maturation. *Proc. Natl. Acad. Sci. USA* **108**, 18436–18441
9. Chan, Y.R., Liu, J.S., Pociask, D.A., Zheng, M., Mietzner, T.A., Berger, T., Mak, T.W., Clifton, M.C., Strong, R.K., Ray, P., and Kolls, J.K. (2009) Lipocalin 2 is required for pulmonary host defense against Klebsiella infection. *J. Immunol.* **182**, 4947–4956
10. Beuckmann, C.T., Aoyagi, M., Okazaki, I., Hiroike, T., Toh, H., Hayaishi, O., and Urade, Y. (1999) Binding of biliverdin, bilirubin, and thyroid hormones to lipocalin-type prostaglandin D synthase. *Biochemistry* **38**, 8006–8013
11. Tanaka, T., Urade, Y., Kimura, H., Eguchi, N., Nishikawa, A., and Hayaishi, O. (1997) Lipocalin-type prostaglandin D synthase (beta-trace) is a newly recognized type of retinoid transporter. *J. Biol. Chem.* **272**, 15789–15795
12. Inui, T., Ohkubo, T., Urade, Y., and Hayaishi, O. (1999) Enhancement of lipocalin-type prostaglandin D synthase enzyme activity by guanidine hydrochloride. *Biochem. Biophys. Res. Commun.* **266**, 641–646
13. Kanekiyo, T., Ban, T., Aritake, K., Huang, Z.L., Qu, W.M., Okazaki, I., Mohri, I., Murayama, S., Ozono, K., Taniike, M., Goto, Y., and Urade, Y. (2007) Lipocalin-type prostaglandin D synthase/beta-trace is a major amyloid beta-chaperone in human cerebrospinal fluid. *Proc. Natl. Acad. Sci. USA* **104**, 6412–6417
14. Inui, T., Ohkubo, T., Emi, M., Irikura, D., Hayaishi, O., and Urade, Y. (2003) Characterization of the unfolding process of lipocalin-type prostaglandin D synthase. *J. Biol. Chem.* **278**, 2845–2852
15. Miyamoto, Y., Nishimura, S., Inoue, K., Shimamoto, S., Yoshida, T., Fukuhara, A., Yamada, M., Urade, Y., Yagi, N., Ohkubo, T., and Inui, T. (2010) Structural analysis of lipocalin-type prostaglandin D synthase complexed with biliverdin by small-angle X-ray scattering and multi-dimensional NMR. *J. Struct. Biol.* **169**, 209–218
16. Inoue, K., Yagi, N., Urade, Y., and Inui, T. (2009) Compact packing of lipocalin-type prostaglandin D synthase induced by binding of lipophilic ligands. *J. Biochem.* **145**, 169–175
17. Iida, T., Nishimura, S., Mochizuki, M., Uchiyama, S., Ohkubo, T., Urade, Y., Tanaka, A., and Inui, T. (2008) Thermal unfolding mechanism of lipocalin-type prostaglandin D synthase. *FEBS J.* **275**, 233–241
18. Jackson, S.E. (1998) How do small single-domain proteins fold? *Fold. Des.* **3**, 81–91
19. Muralidhara, B.K. and Wittung-Stafshede, P. (2004) Thermal unfolding of Apo and Holo Desulfovibrio desulfuricans flavodoxin: cofactor stabilizes folded and intermediate states. *Biochemistry* **43**, 12855–12864
20. Aatif, M., Rahman, S., and Bano, B. (2011) Protein unfolding studies of thiol-proteinase inhibitor from goat (Capra hircus) muscle in the presence of urea and GdnHCl as denaturants. *Eur. Biophys. J.* **40**, 611–617
21. He, G.J., Zhang, A., Liu, W.F., Cheng, Y., and Yan, Y.B. (2009) Conformational stability and multistate unfolding of poly(A)-specific ribonuclease. *FEBS J.* **276**, 2849–2860
22. Meinhold, D.W. and Wright, P.E. (2011) Measurement of protein unfolding/refolding kinetics and structural characterization of hidden intermediates by NMR relaxation dispersion. *Proc. Natl. Acad. Sci. USA* **108**, 9078–9083
23. Mahler, B., Doddapaneni, K., Kleckner, I., Yuan, C., Wistow, G., and Wu, Z. (2011) Characterization of a transient unfolding intermediate in a core mutant of gammaS-crystallin. *J. Mol. Biol.* **405**, 840–850
24. Wishart, D.S., Bigam, C.G., Holm, A., Hodges, R.S., and Sykes, B.D. (1995) 1H, 13C and 15N random coil NMR chemical shifts of the common amino acids. I. Investigations of nearest-neighbor effects. *J. Biomol. NMR.* **5**, 67–81
25. Delaglio, F., Grzesiek, S., Vuister, G.W., Zhu, G., Pfeifer, J., and Bax, A. (1995) NMRPipe: a multidimensional spectral processing system based on UNIX pipes. *J. Biomol. NMR.* **6**, 277–293
26. Matsuura, H., Shimotakahara, S., Sakuma, C., Tashiro, M., Shindo, H., Mochizuki, K., Yamagishi, A., Kojima, M., and Takahashi, K. (2004) Thermal unfolding of ribonuclease T1 studied by multi-dimensional NMR spectroscopy. *Biol. Chem.* **385**, 1157–1164
27. Kuwata, K., Shastry, R., Cheng, H., Hoshino, M., Batt, C.A., Goto, Y., and Roder, H. (2001) Structural and kinetic characterization of early folding events in beta-lactoglobulin. *Nat. Struct. Biol.* **8**, 151–155
28. Sakurai, K., Konuma, T., Yagi, M., and Goto, Y. (2009) Structural dynamics and folding of beta-lactoglobulin probed by heteronuclear NMR. *Biochim. Biophys. Acta.* **1790**, 527–537
29. Kobayashi, T., Ikeguchi, M., and Sugai, S. (2000) Molten globule structure of equine beta-lactoglobulin probed by hydrogen exchange. *J. Mol. Biol.* **299**, 757–770
30. Nakagawa, K., Tokushima, A., Fujiwara, K., and Ikeguchi, M. (2006) Proline scanning mutagenesis reveals non-native fold in the molten globule state of equine beta-lactoglobulin. *Biochemistry* **45**, 15468–15473
31. Yamamoto, M., Nakagawa, K., Fujiwara, K., Shimizu, A., and Ikeguchi, M. (2011) A native disulfide stabilizes non-native helical structures in partially folded states of equine beta-lactoglobulin. *Biochemistry* **50**, 10590–10597
32. The PyMOL Molecular Graphics System. Version 1.3, Schrödinger, LLC